Case Studies in Thermal Engineering 72 (2025) 106306

Contents lists available at ScienceDirect

Case Studies in Thermal Engineering

journal homepage: www.elsevier.com/locate/csite

Recycling waste lubricating oil using two-step pyrolysis and its combustion characterization blended with Jet-A1 in the lean pre-vaporized premixed system

Ahmed I. EL-Seesy [a,b,*], Ahmed S. Attia [b], Radwan M. EL-Zohairy [b], Mohamed I. Hassan Ali [a,**]

[a] Mechanical and Nuclear Engineering Department, College of Engineering and Physical Sciences, Khalifa University, Abu Dhabi, 127788, United Arab Emirates

[b] Mechanical Engineering Department, Benha, Benha Faculty of Engineering, Benha University, 13512, Benha, Qalubia, Egypt

GRAPHICAL ABSTRACT

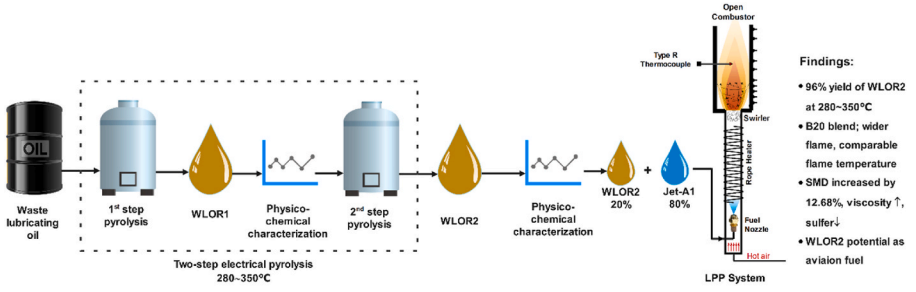

ARTICLE INFO

Keywords:
Waste lubricating oil
Two-step electrical pyrolysis
TGA and FTIR analysis
WLOR2 and Jet A1 blend
Swirl stabilized combustor
Flame temperature assessment

ABSTRACT

This research investigated waste-lubricating-oil (WLO) recycling using a two-step electrical pyrolysis process and then blended the produced oil with Jet-A1 to explore its combustion features in a lean-pre-vaporized-premixed system. The experiment consisted of two parts. The electrical pyrolysis reactor was initially designed and constructed at a laboratory scale. The WLO was then converted to waste-lubricating-oil-round-2 (WLOR2) using the pyrolysis reactor in two rounds. The physicochemical properties of the produced oil were evaluated using FTIR and TGA. In the second part, the flame temperature profiles of pure Jet-A1 and a blend of 20 % by volume WLOR2

* Corresponding author. Mechanical and Nuclear Engineering Department, College of Engineering and Physical Sciences, Khalifa University, Abu Dhabi 127788, United Arab Emirates.

** Corresponding author.

E-mail addresses: ahmed.elsisi@ku.ac.ae (A.I. EL-Seesy), mohamed.ali@ku.ac.ae (M.I. Hassan Ali).

https://doi.org/10.1016/j.csite.2025.106306
Received 11 February 2025; Received in revised form 7 May 2025; Accepted 8 May 2025
Available online 9 May 2025

and 80 % by volume Jet-A1, labeled B20, were evaluated in a lean pre-vaporized premixed system under lean conditions. Results showed that the maximum yield of WLOR2 was around 96.5 %, achieved within a temperature range of 280 ~ 350 °C. The physicochemical properties of the produced oil were comparable to Jet-A1, exhibiting a sulfur content of 0.24 wt%, a viscosity of 3.34 cSt, a cetane index of 60.8, and a heating value of 42,948 kJ/kg. The flame of the B20 blend demonstrated a wider morphology than pure Jet-A1, attained higher temperatures than Jet-A1 at lower levels, and achieved thermal uniformity comparable to that of Jet-A1 at the combustor output.

Nomenclatures

Abbreviation	Meaning
B20	Blend of 20 % WLOR2 plus 80 % Jet A1
WEO	Waste engine oil
WLO	Waste lubricating oil
WLOR1	The produced waste lubricating oil pyrolysis round 1
WLOR2	The produced waste lubricating oil pyrolysis round 2
FT-IR	Fourier transform infrared
GC–MS	Gas chromatography and mass spectrometry
HHV	Higher heating value
LHV	Lower heating value
LPP	Lean pre-vaporized premixed
SMD	Sauter mean diameter
TGA	Thermogravimetric analysis

Symbol	Description	Unit
ΔP_l	Pressure drop of the liquid fuel across the injector nozzle	[Pa]
T_f	Flame temperature	[K]
PF	Pattern factor	–
T_{max}	Maximum recorded temperature	[K]
T_{min}	Minimum recorded temperature	[K]
T_{avg}	Average outlet temperature	[K]
T_i	Incoming air temperature	[K]
R	Radial location from the combustor axis	[mm]
Z	Axial location above the combustor base	[mm]
μ_l	Liquid dynamic viscosity	[Pa.s]
ρ_a	Ambient air density	[Kg/m^3]
σ	Surface tension	[N/m]
φ	Equivalence ratio	–

1. Introduction

The growing global population, industry, and the number of vehicles have led to the availability of huge quantities of waste engine oil (WEO) annually. Automotive lubricating oil constitutes 57 % of the overall worldwide lubricant demand, highlighting its significance across several sectors. [1]. However, approximately 4.4 million tons of WEO are produced every year, with nearly 60 % of this waste being improperly managed or disposed of [1]. The improper handling and burning of hazardous automotive waste releases harmful pollutants, including ammonia, nitric oxide, sulfur dioxide, carbon monoxide, carbon dioxide, and particulate matter, into the atmosphere [2]. Furthermore, WEO has harmful metals like zinc, chlorine, and phosphorus, along with toxic chemicals and polycyclic aromatic hydrocarbons. These substances can seriously harm the environment, human health, soil quality, and marine ecosystems.

To mitigate these environmental and health hazards, various methods for treating waste oil have been developed, including gasification, incineration, hydrothermal liquefaction, and pyrolysis. Among these, pyrolysis has been considered a promising thermochemical conversion process for transforming WEO into a fuel with properties similar to diesel or jet fuel. Pyrolysis produces a fuel with a high level of alkane concentration, a high heating value, and relatively low viscosity, making it a viable alternative for compression ignition engines and potentially for aviation applications [3]. The process involves heating raw materials in an oxygen-free environment, where the C-C and C-H bonds in the polymer are broken, resulting in hydrocarbons of varying lengths. These hydrocarbons are then fractionated to produce an oil-like fuel [4].

In a typical pyrolysis process, raw materials, such as waste plastic or petroleum sludge, are placed in a pyrolysis reactor. Under high temperatures, the heavy structural hydrocarbons decompose and transition into the vapor phase. This method is widely favored due to its efficiency, product quality, cost-effectiveness, and relatively short processing time. Traditional pyrolysis is known for its stability, high product yield, and low production costs. An important factor in the pyrolysis process is temperature, as it directly influences the distribution of solid, liquid, and gas products. Higher temperatures generally favor the production of liquid and gas over solid residues [5,6]. While temperatures of 450 °C or higher are optimal for generating liquid products, lower temperatures are often preferred for specific liquid product formulations [7]. A critical step in the process is the removal of water from the pyrolysis fluid to enhance its

quality [8]. The resulting pyrolysis fluid, which varies in color and composition depending on the feedstock, is commonly referred to as oil, bio-oil, or tar. Among the various pyrolysis techniques, electrical pyrolysis, thermal pyrolysis, and microwave-assisted pyrolysis are the most commonly used for converting WEO into fuels with diesel or fuel-like jet. Electrical pyrolysis, in particular, has gained attention due to its lower energy consumption, moderate heating rates, and cost-effectiveness compared to microwave-assisted pyrolysis.

Several factors influence the efficiency and outcome of the electrical pyrolysis process, including pyrolysis temperature, heating rate, residence time, and pressure [9]. These factors significantly affect the yield and quality of the pyrolysis products. For instance, increasing the heating rate tends to reduce char yield while enhancing the production of gas and liquid. Similarly, elevated pyrolysis temperatures raise the quantity of the produced gas but reduce char yield and reactivity [10]. Residence time and pressure also play significant roles in determining the yield and reactivity of the resulting char. Specifically, longer residence times increase char yield but decrease its reactivity, while higher pyrolysis pressure raises the yield of char and CO_2 but reduces the yield of CO, CH_4, and H_2 [11]. However, the nature of the biomass feedstock has no significant effect on the yield or reactivity of the char.

Gunerhan et al. [12] produced bi-oil from plastics and waste tires using pyrolysis and investigated their combustion characteristics in a gas turbine. It was reported that pyrolysis oils generated from plastic waste and used tires demonstrated stable combustion characteristics and that their CO and HC emissions were comparable to those of commercial jet fuel. However, they reported that enhancing pyrolysis oil viscosity, moisture content, and aromatic composition could improve their viability as alternative aviation fuels. These improvements could contribute to the aviation sector's carbon neutrality by encouraging the competitiveness of pyrolysis oils relative to conventional jet fuels. Likewise, Santiago et al. [13] assessed the conversion of oil sludge throughout the gasification process and applied it to a gas microturbine. It was determined that gasification was identified as a promising technology for oil sludge management and treatment. The process allows for the production of fabricator gas, which can be used for electricity generation, while significantly reducing environmental impact compared to conventional methods like incineration.

Suchocki et al. [14] produced bio-oil from waste tires using pyrolysis and applied it to a gas turbine to asses its combustion and emission parameters. They mentioned that adding waste oil somewhat increased turbine inlet and outlet temperatures. It was noted that there was an increase in values of thrust-specific NO_x and CO levels for the gas turbine fuelled by waste oil/kerosene. Meanwhile, levels of SO_2 were lower for all tested waste oil/kerosene combinations than for pure kerosene. Applying bio-oil in heater combustion systems or gas turbines produced through pyrolysis from waste plastic was performed by Wang et al. [15], Broumand et al. [16], and Seljak et al. [17]. It was noticed that waste oil could be applied directly in gas turbines or burners. The authors emphasized the necessity of fuel supply system modifications for enhanced operational flexibility. Furthermore, they highlighted that injector modifications or waste oil upgrades would be required before commercial applications.

The Lean Premixed Prevaporized (LPP) combustion system, recognized for its superior fuel-air mixing and enhanced combustion efficiency, provides an advantageous platform for evaluating alternative fuels. This study demonstrated the potential of waste lubricating oil (WLO)-derived fuel as a viable renewable aviation fuel, addressing critical environmental concerns associated with waste oil disposal. By integrating waste management strategies with sustainable energy solutions, this research contributes to developing environmentally sound and economically viable alternatives for both aviation and broader combustion applications, thereby advancing the transition towards a more sustainable energy future. Gunerhan et al. [12], Chiong et al. [18], Broumand et al.

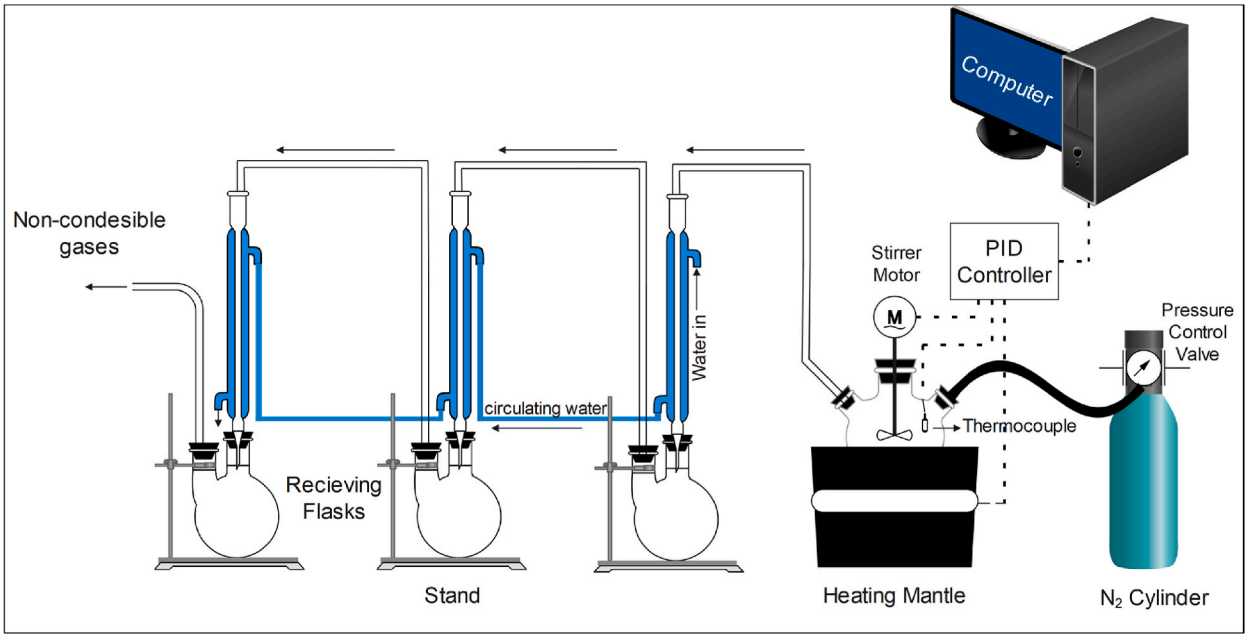

Fig. 1. The simplified diagram of the pyrolysis system.

[19], and Shahbaz et al. [20] recommended that future research prioritize fuel upgrading strategies when assessing the viability of pyrolysis oils for aviation applications. Future research should explore methods for upgrading pyrolysis oils to ensure compliance with environmental regulations and mitigate potential ecological impacts.

While some researchers have investigated bio-oil production from waste sources such as cooking oil, biomass, and other waste feedstocks, a comprehensive study examining the two-step pyrolysis of waste lubricating oil (WLO) and its subsequent combustion characteristics in external combustion systems (e.g., gas turbines, burners, heating systems) remains lacking. This investigation addresses this gap by employing a two-step electrical pyrolysis process to convert WLO into bio-oil (WLOR2) and evaluating the combustion parameters of WLOR2 blended with Jet A1 in a Lean Premixed Prevaporized (LPP) system. The experimental methodology comprised two principal stages: (i) designing and constructing a laboratory-scale electrical pyrolysis reactor. Thermogravimetric analysis (TGA) of the raw WLO informed the selection of heating elements, temperature control systems, and other reactor components. The pyrolysis process yielded bio-oil, designated WLOR1 after the first stage and WLOR2 after the second. WLOR2 was characterized using TGA, Fourier Transform Infrared Spectroscopy (FTIR), and Gas Chromatography-Mass Spectrometry (GC-MS). Physicochemical properties were measured following ASTM standards and compared with those of Jet A1. (ii) A 20 % (by volume) blend of WLOR2 with Jet A1 was then prepared to assess its influence on the combustion parameters within the LPP system.

2. Materials and methodology

The first part of the subsequent section illustrates the preparation process of fuel-like diesel. The LPP system and the measurement technique are subsequently described in the second part. Afterward, the experimental program and testing procedures employed to conduct this investigation are demonstrated in the last part of this section.

2.1. Electrical pyrolysis system for waste lubricating oil

This section provides a brief explanation of the system components used for fuel production and the operational procedures. Fig. 1 depicts the schematic diagram of the pyrolysis system employed in the current investigation. A pyrolysis reactor was constructed for the production of liquid fuel from waste lubricating oil. The reactor is configured as a spherical fixed-bed reactor. The upper section of the reactor may be opened for the introduction of raw oil, and there is a stirring motor to agitate the oil. A heating mantle with a power capability of 380 W and a maximum temperature of 450 °C is used to provide the necessary heat during the procedure. The reactor's temperature is continuously monitored using a type K thermocouple connected to a data acquisition system. To maintain an inert atmosphere, pure nitrogen (99.99 %) is supplied at a flow rate of 2.5 L/min throughout the process. Three volatile condensers are provided for the condensation of volatile gases, referred to as WLOR1 or WLOR2. Hot gases traversed the inside of the condenser tube and condensed with the aid of circulating room-temperature water enveloping the tube. Some gases, including CH_4, H_2, CO_2, and light hydrocarbons, are not condensable and can be released through a vent tube [21]. The produced oil may be extracted from three receiving flasks, each with a capacity of 0.5 L.

To produce the required amount of the fuel, the following procedures are followed:

1 Measuring 650 mL of WLO and pouring it into the three-neck, round-bottom flask.
2 Placing the flask on the heating mantle and gradually adjusting the temperature across a range of 250, 300, 350 °C, and up to 430 °C at a temperature rate of 5 °C/min.
3 Adjusting the nitrogen flow at 2.5 L/min using the pressure valve.
4 Allowing for the water to circulate in the water-cooled condenser to condense the vapor produced during the pyrolysis.
5 Monitoring and controlling the process temperature using the DAQ.
6 The produced liquid fuel, referred to as WLOR1, is collected from three receiving flasks and analyzed for its physical and chemical properties.
7 WLOR1 undergoes a second pyrolysis process, resulting in a refined product termed WLOR2.

Table 1 summarizes the pyrolysis process conditions for waste lubricating oil. To validate the potential of WLO-derived fuel for LPP applications, WLOR2 was blended with Jet A1 at a ratio of 20 %. The blended fuel was then tested in an LPP system to evaluate its combustion characteristics and temperature behavior.

2.2. LPP setup and measurement techniques

An LLP test rig was employed to carry out this investigation, as depicted in Fig. 2. The diagram illustrates that pressurized air is supplied by a large storage tank via a screw compressor, MSK G22, to an air heating system consisting of two-stage heating lines. The

Table 1
The operating conditions of producing WLOR1 and WLOR2.

Raw oil	Stage	Process temperature	Process time (h)	Yield%	Sulfur content	Viscosity (cSt)	Product
WLO	Round 1	30-450 °C; highest yield at 350–400 °C	4	82.5	1.95 % wt.	4.73	**WLOR1**
WLOR1	Round 2	30-450 °C; highest yield at 280–350 °C	3.25	96.5	0.24 % wt.	3.34	**WLOR2**

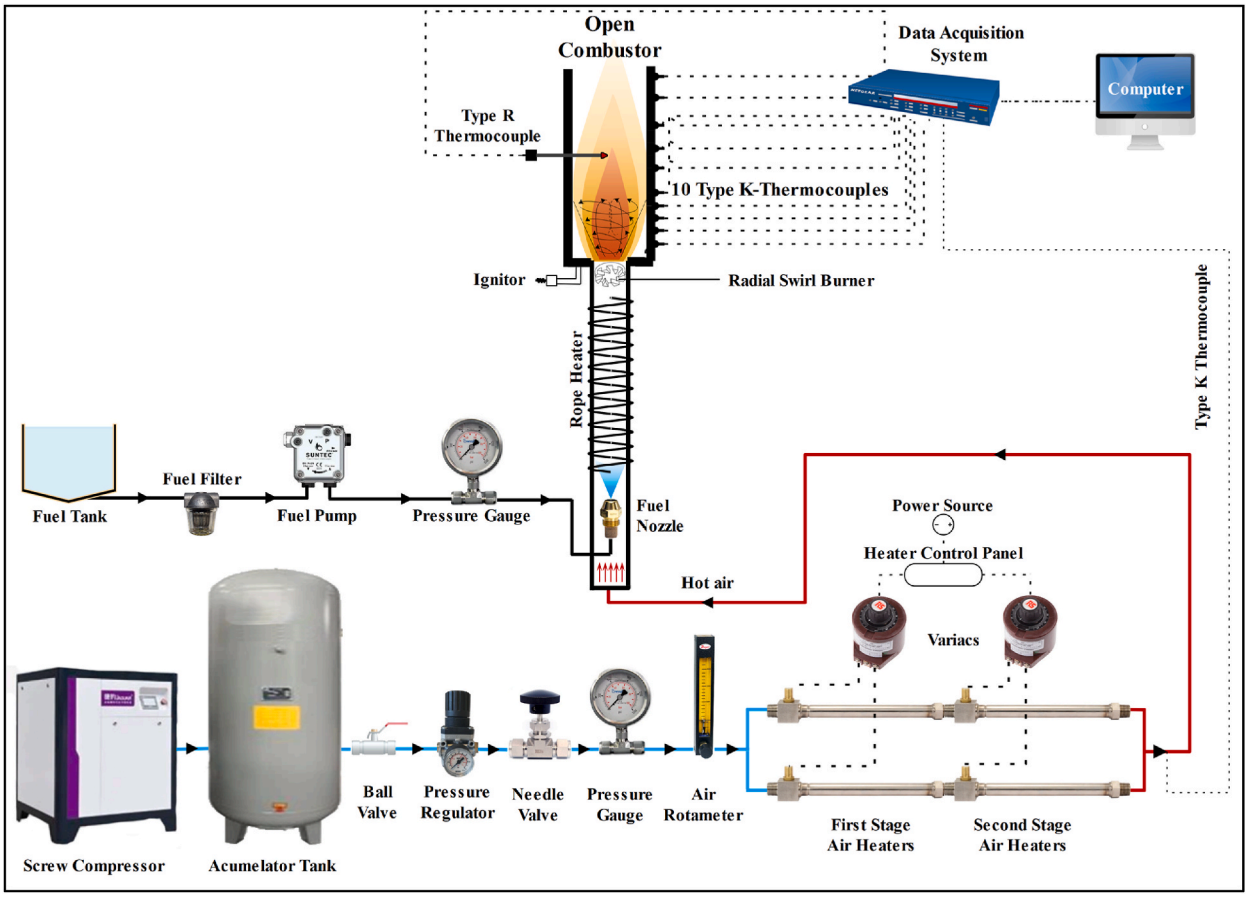

Fig. 2. Schematic diagram of the test rig.

initial stage has two heaters with a maximum heating load of 2400 W, while the second stage has a heating load of 1500 W. Both of them are regulated by variable voltage transformers based on the output air temperature, which is monitored by a thermocouple type K. The airflow rate is adjusted by a pressure control valve and measured using a high-flow glass flowmeter – DR4, situated just before the heating system.

The evaluated fuel is pumped from the tank by a gear pump, SUNTEC AL35, at the required pressure for the oil nozzle to atomize it inside the section tube effectively. The fuel nozzle generates a solid 45° cone spray with a specified flow rate of 0.6 gallons per minute. The atomized fuel combines with the incoming heated air in the mixing tube, whose dimensions and details are indicated in Fig. 3, creating a combustible air-fuel mixture that is ready for ignition upon entering the combustion chamber. A radial swirl burner of 1.61 cm diameter and 0.55 swirl number is employed to enhance the mixing degree between air and fuel by generating a swirling motion. The mixing tube is further enclosed by an insulating layer and fitted with a rope heater to mitigate heat loss and sustain the internal temperature at the specified levels. A 24 kV high-voltage ignitor serves to ignite the combustible mixture once it enters the combustor, which has a diameter of 15 cm and a height of 50 cm. The combustor is constructed from steel and is equipped with measuring ports and slots to allow the measuring element to be inserted into the flame without air entrainment.

The temperatures of the flame are measured using a precalibrated type R thermocouple with ceramic tube insulation, exhibiting an accuracy of 1.5 °C. Furthermore, a data acquisition was implemented to record all thermocouple signals autonomously. Due to the thermal radiation that reaches the combustion chamber wall, the El-Zoheiry approach [22] was utilized to correct all recorded data for the heat losses attributed to this radiation. The flame temperatures through the combustion zone were measured at 112 locations, and the wall temperature was measured at ten locations, as depicted in Fig. 4. A 2-D traverse mechanism was employed to support the thermocouple rod throughout the measurement procedures.

The range of estimated errors in a given measurement is called uncertainty (U). The following equation expresses the uncertainty of Result R, according to Kline [23]:

$$U_R = \sqrt{\left(\frac{\partial R}{\partial v_1} U_{v_1}\right)^2 + \left(\frac{\partial R}{\partial v_2} U_{v_2}\right)^2 + \ldots + \left(\frac{\partial R}{\partial v_n} U_{v_n}\right)^2}$$

Where v_1, v_2, and v_n denote the measured readings. The flame temperature is subjected to an uncertainty analysis in this study, with a

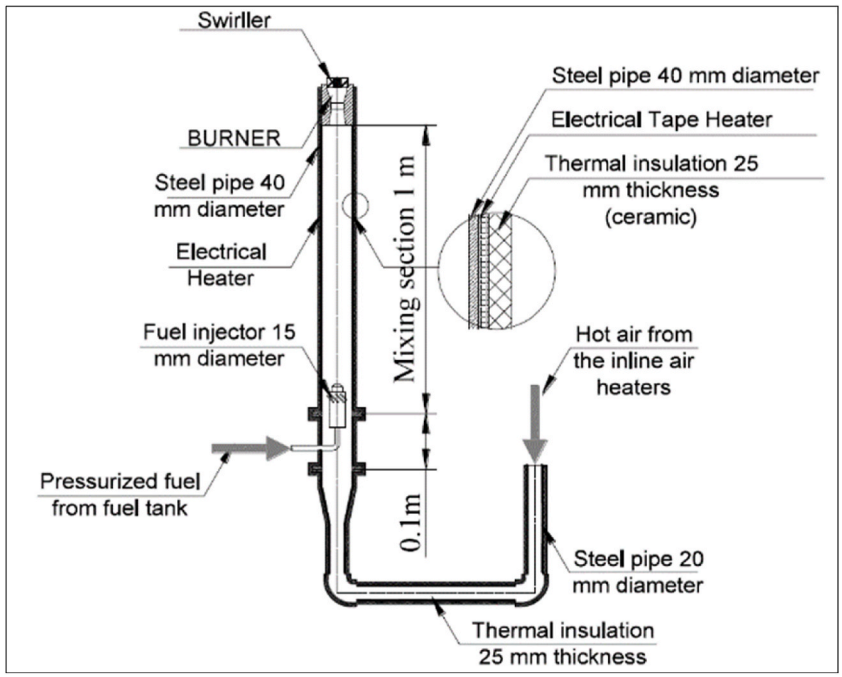

Fig. 3. Details of the mixing section.

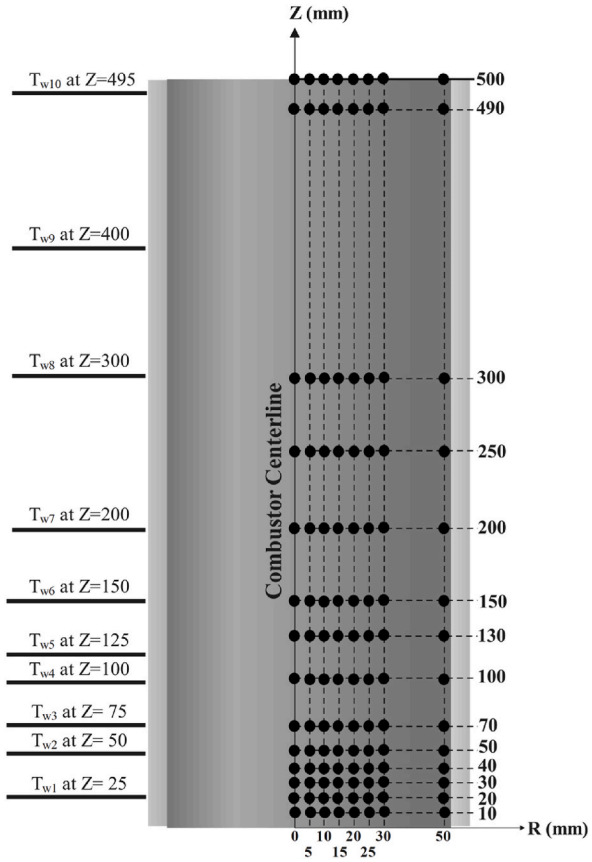

Fig. 4. Coordination of wall thermocouples and flame temperature sampling locations.

maximum uncertainty of 0.735 %.

2.3. Experimental program and testing procedures

Before conducting the intended investigation, an experimental program was established. The same operating parameters, such as an equivalence ratio of 0.85, are achieved by maintaining air and fuel flow rates. Additionally, the air temperature is kept at 350 °C. Values of the experiment parameters are presented in Table 2.

In order to carry out the experiments, specific procedures are implemented. The first step is to drain the compressor tank of any accumulated moisture. Then, the compressor is started after adjusting the specified pressure range. After that, the airflow rate is set to the target value using the rotameter and pressure gauge. The next step is to activate the heating system and set the variable transformers to obtain the desired temperature. Afterward, the oil pump is started and set to the required pressure using the online flow rate measurements. After ensuring that the appropriate equivalence ratio is reached, the combustible mixture is initiated with the high-voltage ignitor to commence combustion. Once the combustor wall temperature stabilizes, the 2-D supporting mechanism measures the flame temperatures at specific spots.

3. Results and discussion

This section provides a discussion about the physical and chemical properties, TGA results, GC-MS, and FTIR for WLOR2 in sections 3.1 and 3.2. Section 3.3 evaluates the combustion of the B20 blend in comparison to Jet A1. Section 3.3 summarizes and compares the waste lubricating oil produced using the pyrolysis method with findings from other related studies.

3.1. Characterization of the produced WLO and its blend with Jet A1

The oils produced from the pyrolysis of raw waste lubricating oil are evaluated using thermogravimetric analysis (TGA) and Fourier transform infrared spectroscopy (FTIR). Fig. 5 (a) presents the TGA results for both tested fuels obtained using a Setaram LABSYS EVO TG-DTA/DSC at 1600 °C. Fig. 5(a) and (b) illustrate that WLOR1 gradually vaporizes around 120 °C, with total vaporization occurring at roughly 400 °C. Conversely, WLOR2 starts to evaporate gradually at about 120 °C and is entirely vaporized by 300 °C, with no residual mass at 500 °C, when compared to the raw WLO. The results demonstrate that the two-step pyrolysis process significantly improves oil volatility. FTIR analysis further supports this trend, which indicates a shift toward lower boiling point components in WLOR2 than in WLOR1, as shown in Fig. 5 (b).

FTIR spectroscopy was performed to identify the presence of essential functional groups at WLOR1 and WLOR2, as illustrated in Fig. 5 (b) and Table 3. FTIR spectroscopy was conducted to identify the key functional groups present in WLOR1 and WLOR2, as seen in Fig. 5 (b) and Table 3. The peak at 2921.7 cm^{-1} corresponds to C–H stretching, whereas the peak at 1738.91 cm^{-1} is associated with C=H bending, as shown in Fig. 5 (b). The FTIR profile demonstrates that the predominant hydrocarbons detected in WLOR2 are alkanes and C=H bending alkenes. The results align with those reported by Lam et al. [24].

The composition of WLOR2 is analyzed using GC-MS with a QP2010ULTRA model, including a 5 ms column. Fig. 6 shows specific peaks in the GC−MS chromatogram, which correspond to the components of the produced oil on the basis of their retention times and fragmentation patterns. GC−MS analysis indicated that WLOR2 mostly contains straight-chain alkanes with carbon numbers between 9 and 28, as shown in Table 4. The identification of these components can be verified by comparing their retention times and mass spectra with the results presented by Maceiras et al. [25].

3.2. Physicochemical properties of the tested fuels

Table 5 presents the physicochemical properties of Jet A1, WLO, WLOR1, and WLOR2 produced from WLO by an electrical pyrolysis process. These properties are determined at the Egyptian Petroleum Research Institute (EPRI-Central Analytical Labs, Nasr City, Cairo, Egypt) using standard methods outlined by the American Society for Testing and Materials (ASTM). As indicated in Table 5, the density of WLOR2 slightly exceeds that of Jet A1, while its viscosity is about 3 times that of Jet A1. The distillation curve for WLOR2 is greater than that of Jet-A1, possibly due to the difference in chemical bonds between Jet-A1 and WLOR2.

Furthermore, Table 5 lists the physical parameters of the tested fuels. The fuel density is measured at 20 °C using a METTLER TOLEDO DM40 density meter, while the viscosity is evaluated at 40 °C using an Ostwald viscometer. Table 5 indicates that WLOR2 has viscosity and density values slightly higher than those of Jet A1. The caloric value of WLOR2 is approximately 1.6 % lower than that of Jet A1.

Fig. 7 reflects the volatility of the fuels, aiding the selection of an appropriate air temperature to ensure fuel vaporization. TG analysis quantifies the rate and extent of mass variation of a substance in relation to temperature variations. A Labsys Evo-Setaram

Table 2
Experimental operating conditions.

Fuel Type	Fuel Flow [kg/h]	Air Flow [kg/h]	Air Temp. [°C]	Equivalence Ratio [−]
Jet-A1	1.23	21.04	350	0.85
B20	1.27	21.04	350	0.85

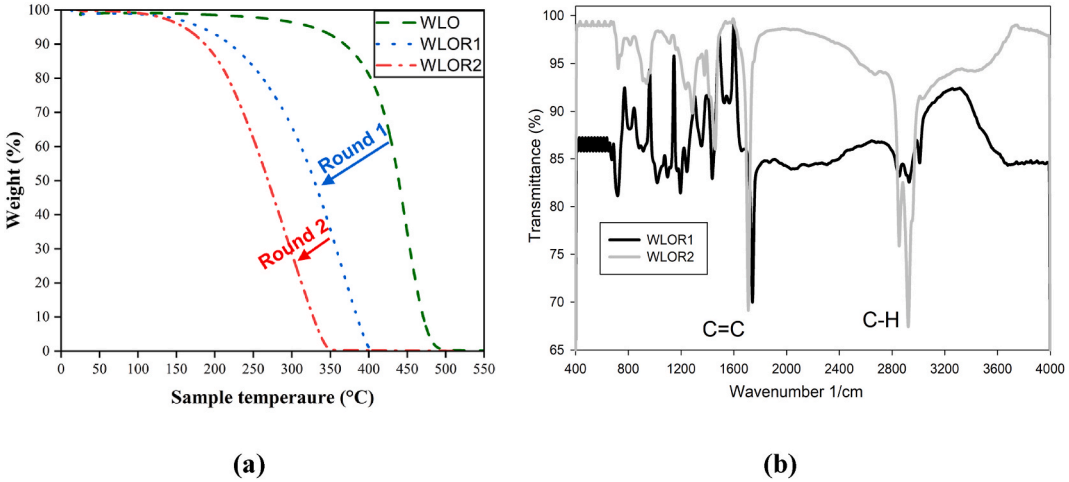

Fig. 5. TGA and FTIR results for both raw oil and produced oils produced from the pyrolysis process.

Table 3
FTIR functional groups identified in WLOR1 and WLOR2.

Frequency range (cm^{-1})	Functional clusters	Category of compounds
3200–3400	O – H stretching	Alcohols, phenols, or carboxylic acid
2750–3000	C – H stretching	Alkanes
1700–2100	C = O stretching	Aldehydes, ketones, or carboxylic acid
1575–1675	C = C stretching	Alkenyl
1345–1500	C = H bending/deformation	Alkenes
900–1200	C = H bending	Alkenes
675–850	C – H out-of-plane bending	Single-ring aromatics

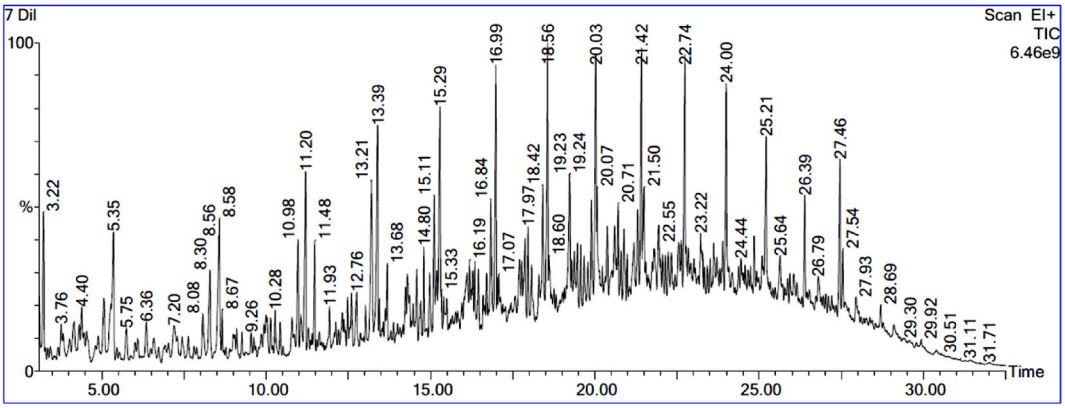

Fig. 6. Gas chromatogram for WLOR2.

analyzer was used to conduct these tests. The TGA line chart indicates that Jet A-1 begins evaporation at 150 °C and fully evaporates at 260 °C. WLO commences evaporation at around 300 °C and completes the process at around 480 °C, while WLOR1 begins evaporation at around 150 °C and concludes at roughly 400 °C. In contrast, WLOR2 begins evaporation at around 150 °C and achieves complete evaporation at 350 °C. Considering that the WLOR2 sample completely evaporates at about 350 °C, an air preheating temperature of 350 °C was selected, and a steady flame was attained by maintaining the equivalence ratio at a lean state of 0.85.

3.3. Flame evaluation

In the field of combustion, the temperature within the flame is a significant parameter essential for understanding combustion features. Fig. 8 presents a contour plot of the flame temperature, offering a detailed depiction of the temperature of the flame zone. As depicted in the illustration, the flame can be divided into three distinct zones. The first zone is the flame initiation zone, which initiates

Table 4
Main compounds obtained from the WLOR2 sample.

Compound Name	Mass %	Molecular Formula
Heneicosane	12.04	$C_{21}H_{44}$
Eicosane	8.49	$C_{20}H_{42}$
Nonadecane	8.24	$C_{19}H_{40}$
Hexadecane	7.04	$C_{16}H_{34}$
1-Nonadecane	6.67	$C_{19}H_{40}$
Octadecane	6.65	$C_{18}H_{38}$
Pentadecane	5.78	$C_{15}H_{32}$
1-Pentadecane	5.21	$C_{15}H_{32}$
Octacosane	5.08	$C_{28}H_{58}$
1-Chloroeicosane	4.51	$C_{20}H_{41}Cl$
Decane	3.56	$C_{10}H_{22}$
heptadecane	3.25	$C_{17}H_{36}$
Tridecane	3.24	$C_{17}H_{28}$
Tetradecane	3.22	$C_{14}H_{30}$
1-Tetradecane	2.93	$C_{14}H_{28}$
Undecane	2.89	$C_{11}H_{24}$
Dodecane	2.77	$C_{12}H_{26}$
Docosane	2.31	$C_{22}H_{46}$
Octadecanal	2.15	$C_{18}H_{36}O$
1-Hexadecene	2.01	$C_{16}H_{32}$
Nonane	1.98	C_9H_{20}

Table 5
Properties of the investigated fuels.

Test	Jet A1	Raw WLO	WLOR1	WLOR2
HHV, KJ/kg	–	–	–	45,600
LHV, KJ/kg	43,640	39,063	–	42,948
C, wt%	86.51	–	–	87.15
H, wt%	13.48	–	–	12.58
O, wt%	Nil	–	–	–
N, wt%	Nil	–	–	0.02
S, wt%	Nil	–	1.95	0.24
Density @ 20 °C, kg/m^3	797	881	841	837.1
Pour point, °C	−43	–	–	−5
Flash point, °C	39	–	–	110
Kinematic viscosity @ 40 °C, cSt	1.08	38	4.73	3.34
M.W, kg/kmol	148.0	–	–	158.19
Initial B.P., °C	150	–	–	149
50 %	210	–	–	310
90 %	250	–	–	350

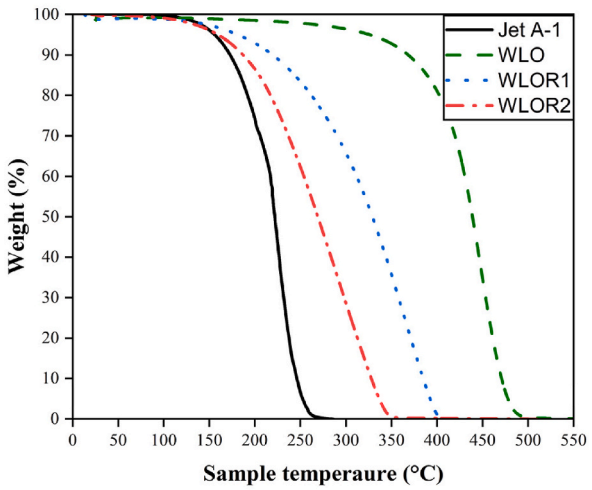

Fig. 7. TGA results of the tested fuels.

the oxidation of premixed reactants. In this region, free radicals are concentrated due to the thermal disequilibrium state of the reactants [26]. This region appears above the burner plan, as illustrated in Fig. 4, measuring approximately 20 mm in length. The oxidizing rate maintains its increase throughout this region, reaching its peak in the subsequent area characterized by severe temperature gradients. The second region is known as the recirculation zone, where maximum temperatures are achieved at around 40 mm from the burner surface. The third region is termed the post-flame zone, when the flame temperature starts to drop due to heat losses from the combustor wall, resulting in the slow extinction of the flame, and it can be found at 240 mm from the burner surface. In other words, the combustion is complete beyond 240 mm above the burner, where the flame gradually diminishes and ultimately dissipates. Fig. 8 illustrates that the flame temperature distribution of the B20 blend is wider than that of Jet A1 at lower elevations, indicating that WLOR2 significantly influences both the flame shape and its temperature distribution.

The flame temperatures are shown as a function of radial locations at various elevations within the combustion chamber, as depicted in Fig. 9. The flame temperatures are observed to exhibit relatively low values at early levels where the initiation reactions are ongoing. This bottom zone is mainly influenced by two reaction processes (branching and initiating), resulting in an increase in the temperature until it hits its peak in the recirculation region created by the swirler. Subsequently, the increasing dominance of product reactions drives the gradual stabilization of the system. The temperature peak values achieved are 2074 K and 2048 K for Jet A1 and the B20 blend, respectively, and they are found at a distance of 40 mm from the burner base. The flame temperature is primarily influenced by the heat of combustion, hydrogen-to-carbon proportion, oxygen concentration, viscosity, and the level of atomization and evaporation attained by the fuel particles before entering the flame zone. Although waste lubricating oil has a lower heat of combustion than Jet A1, the B20 blend reliably generates a higher flame temperature that reaches up to 70 mm above the burner, reflecting more intense initial combustion attributed to the slower evaporation rate of the WLOR2. At higher levels, the temperature gradients of the B20 blend start to flatten, indicating less flame intensity and better thermal homogeneity, maintaining slightly higher values than Jet A1. A potential reason is that the waste lubricating oil was inadequately atomized, leading to fuel droplets lacking sufficient energy and time for complete vaporization prior to entering the flame zone. Consequently, partial diffusion combustion develops at the surface of droplets under stoichiometric conditions when these droplets interact with oxygen in the combustion chamber, resulting in a flame temperature that exceeds that of lean combustion of Jet A1. The droplets resulting from insufficient atomization are considerably denser, preventing the incoming air's inertia from transporting them axially within the combustion chamber, despite the swirler's generation of angular momentum. Consequently, they generate hot spots on the combustor wall by radially escaping towards the wall, where the layers of unevaporated fuel droplets evaporate due to heat transfer from the hot combustion gases on the interior surface of the combustor. At elevated levels, the WLOR2 droplets eventually vaporize, disintegrating the heterogeneous mixture; the mixture attains greater homogeneity, and the flame temperature distribution approaches that of Jet A1, as illustrated in Fig. 9. Another potential reason is that WLOR2 has a greater molecular weight, a bulkier molecular structure, and a higher flash point, contributing to its reduced volatility properties. This is supported by the FTIR results in Fig. 5 and Table 3, which elevate the adiabatic flame temperature [27,28]. These findings are in line with those of Kumar et al. [29] and Chiong MC et al. [30].

The combustor wall temperature is influenced by different fuel blends, despite maintaining the operating conditions for both tested fuels. Fig. 10 indicates that the wall temperature escalates and attains a maximum, resulting in hot spots at the wall caused by the extreme heat concentration at this location. Subsequently, it commences a slow decline till reaching the combustion chamber outlet, as illustrated in Fig. 10. The addition of WLOR2 to Jet A1 elevates the wall temperature, resulting in a divergence from the Jet A1 trend. The highest values recorded were 830.9 K for the B20 blend at 150 mm above the burner, followed by Jet A1 at 779.8 K at 250 mm above the burner. This is because WLOR2 exhibits inadequate atomization, resulting in bigger droplet sizes that lack sufficient period or energy for vaporization before reaching the flame zone. Rather than being axially directed by the incoming air, these heavy droplets are radially forced toward the wall, leading to a partial diffusion combustion mode near it under stoichiometric conditions at the surface. This phenomenon results in a higher peak temperature compared to the lean combustion of Jet A1, consequently elevating the wall temperature.

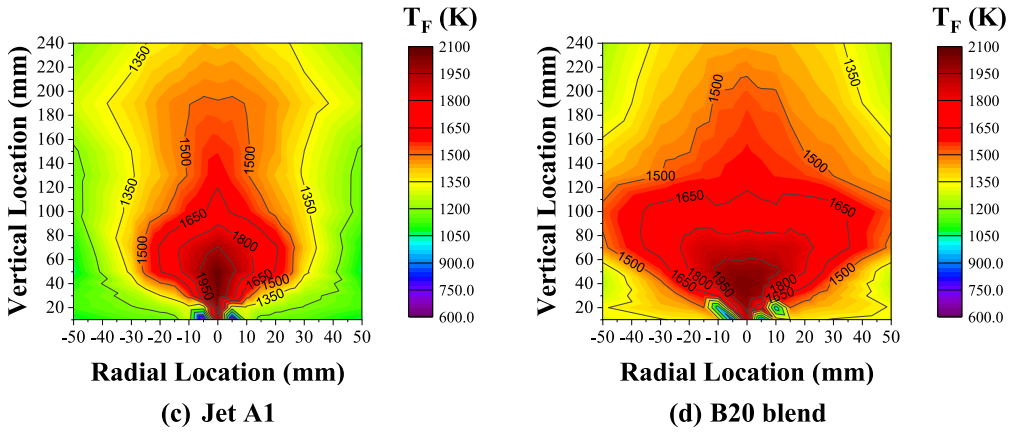

Fig. 8. Contour plot of the flame temperature within the combustor.

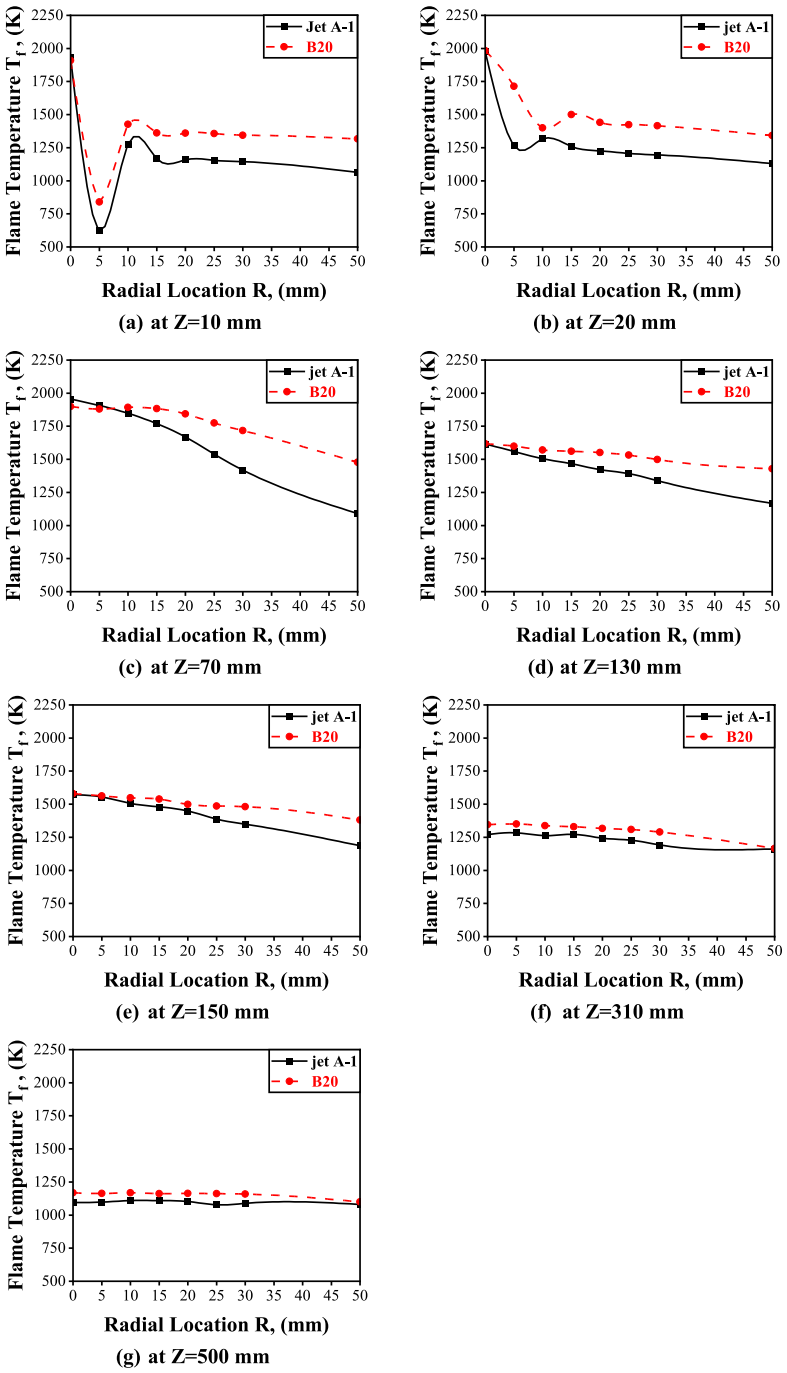

Fig. 9. Radial temperature distribution of the B20 blend compared to Jet A1 within the combustor.

The most appropriate parameter for characterizing the extent of atomization is the Sauter mean diameter (SMD), defined as the mean size of atomized fuel droplets. It indicates the degree of fuel atomization. A smaller Sauter mean diameter correlates with an improved atomization process. The most precise technique for measuring the SMD of fuels is the utilization of a Phase Doppler Particle Analyzer system [31]. Due to financial limitations, a developed SMD formula is utilized to evaluate the SMD size for this research objective [32]. SMD of both tested fuels directly from the nozzle is calculated according to the empirical formula made by Lefebvre and Ballal [32]:

$$SMD = 2.25\sigma^{0.25}\mu_l^{0.25}\rho_a^{-0.25}\Delta P_l^{-0.5}m^{0.25}$$

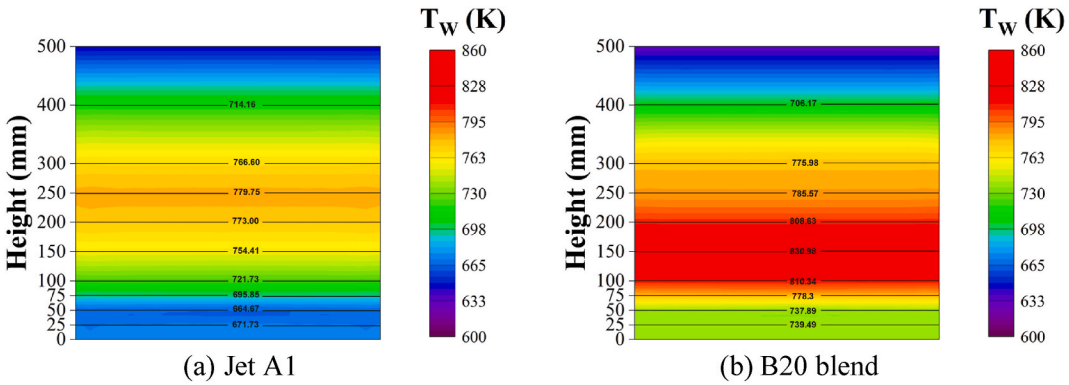

Fig. 10. Wall surface temperature.

The formula employed to compute SMDs provides a comparable trend between both tested fuels rather than getting highly precise SMDs, which are only measured through a comprehensive phase Doppler particle analyzer system [33]. High viscosity limits the instabilities necessary for the fuel jet's fragmentation and hinders the fuel's agitation, leading to an increased SMD and hence, delaying the atomization process. High-viscous fuels have a reduced number of droplets due to the breakup frequency in comparison to diesel fuel [34]. In other words, with an equivalent volume of fuel sprayed via the atomizer, a fewer number of droplets will yield a greater SMD. Thus, it can be deduced that the breakup characteristic is significantly influenced by both surface tension and the internal friction flow within a droplet [35]. An increase in fuel density negatively impacts atomization by impeding the fuel acceleration, whilst greater surface tension hinders droplet creation from the liquid fuel, as previously noted [32].

SMD mainly depends on the surface tension, dynamic viscosity, pressure drop across the injector nozzle, and mass flow rate. Since the operating conditions are identical for both tested fuels, the chemical properties of fuels, such as surface tension and viscosity, are the primary factors influencing the degree of atomization between Jet A1 and the B20 blend. Jet A1 attained a Sauter mean diameter of 8.071 μm, whereas the B20 blend recorded 9.094 μm. This means that the particle size of the B20 blend has increased by 12.68 %. The increased viscosity and density are responsible for the greater SMD of WLOR2 because the viscosity is the primary factor influencing the SMD, as demonstrated [36]. Jet A1 exhibits 0.0265 N/m liquid surface tension compared to 0.0311 N/m for WLOR2. Moreover, Jet A1 has a liquid dynamic viscosity of 0.0008 kg/m.s, whereas WLOR2 has a viscosity of 0.0033 kg/m.s. This corroborates the hypothesis that the morphology of the B20 blend flame observed in Fig. 8 results from the inadequate atomization of the WLOR2.

To demonstrate the uniformity of flame temperature within the combustion chamber, the combustor pattern factor (PF) is calculated across the chamber using the following equation and is presented in Fig. 11. A lower PF indicates better thermal homogeneity within the combustor.

$$PF = \frac{T_{max} - T_{min}}{T_{avg} - T_i}$$

As shown in Fig. 11, the pattern factor profile of both tested fuels commences with a substantial value and subsequently drops progressively until the combustor outlet. The B20 blend has a lower pattern factor than Jet A1. This is a consequence of the WLOR2 droplet combustion in the lower levels of the combustor.

3.4. Summary of waste lubricating oil production and combustion assessment

Table 6 summarizes the waste lubricating oil production by the pyrolysis process used in this current study and related published works. The properties of waste oil feedstocks, particularly the sulfur content, significantly influence the pyrolysis process parameters. The maximum yield was achieved at temperatures ranging from 300 to 350 °C, whereas the current investigation indicates yields of 350 ~ 400 °C for WLOR1 and 280 ~ 350 °C for WLOR2. In the same way, the amount of sulfur in the oil determines whether one-stage or two-stage desulfurization is used to lower the sulfur level after the pyrolysis process. The viscosity and heating value of the fuel oil produced in this study are comparable to those reported in the literature. Moreover, this study achieved better oil yields, recording 82.5 % for WLOR1 and 96.5 % for WLOR2.

4. Conclusions

This work involved recycling waste lubricating oil through a two-step electrical pyrolysis reactor at the laboratory scale to produce fuel-like diesel. The design and installation of the pyrolysis reactor were executed first to attain this objective. Similarly, the raw waste lubricating oil was transformed into bio-oil (WLOR2) using electrical pyrolysis, utilizing NaOH (1 wt%) as a catalyst. The produced WLOR2 was further analyzed and blended with Jet A1 at a volume percentage of 20 % to assess its combustion characteristics in premixed combustion in a swirl-stabilized. The physicochemical characteristics of the produced oil were considered using FTIR and TGA. Key findings from this study include:

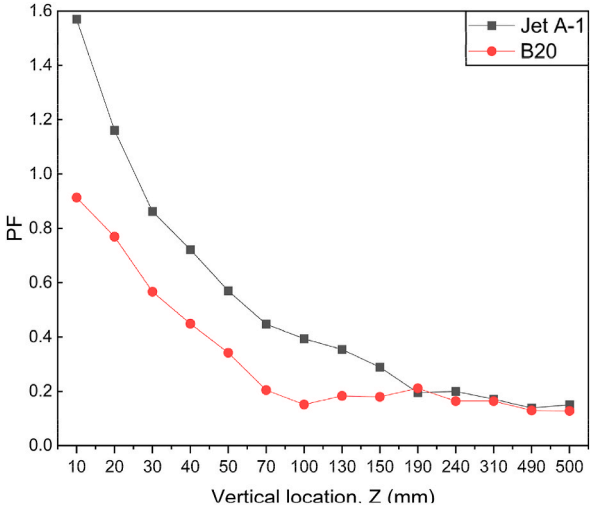

Fig. 11. Combustor pattern factor for both evaluated fuels.

Table 6
Comparison of waste lubricating oil production between the current study and relevant previous works.

Ref.	Production technique	Catalyst and concentration	Process temperature and duration	Yield % wt.	Sulfur [ppm]	Viscosity [cSt]	Heating value [kJ/kg]
[37]	One-stage catalytic pyrolysis	Lime (CaO), 2 % wt.	Up to 500 °C (4 h)	60	3500	3.49	42,500
[38]	Single-stage pyrolysis with an oxidative desulfurization technique	Hydrogen peroxide and formic acid	Up to 420 °C (4 h)	–	4200	3.2	42,100
[39]	One-stage catalytic pyrolysis	Waste cooking oil (0, 10, 20, 30, 50, 75, and 100 %)	Up to 450 °C	73	From 1269 to 5584	–	–
Current study	Two-stage pyrolysis	No catalyst	WLOR1 30 ~ 450 °C (4 h); highest yield at 350 ~ 400 °C	82.5	1.95 % wt.	–	–
			WLOR2 30 ~ 450 °C (3.25 h); highest yield at 280 ~ 350 °C	96.5	0.24 % wt.	3.34	42,948

1. The maximum yield of WLOR2 using two-step pyrolysis was around 96.5 %, achieved within a temperature range of 280 ~ 350 °C. This demonstrated an approximately 18 % increase in oil yield and about a threefold reduction in sulfur content compared to related published studies.
2. The physicochemical properties of the produced oil were comparable to Jet A1, with a sulfur content of 0.24 wt%, a viscosity of 3.34 cSt, a cetane index of 60.8, and a heating value of 42,948 kJ/kg.
3. The B20 blend produced an average SMD of 9.094 μm compared to 8.071 μm for Jet A1, reflecting an increase of 12.68 %.
4. The addition of WLOR2 altered the temperature distribution across the flame, and flame visualization indicated a wider and more stable flame shape for the B20 blend than for Jet A-1.
5. The addition of WLOR2 affected the combustor wall temperature, resulting in a higher peak wall temperature of 830.9 K at Z = 150 mm above the burner for the B20 blend.
6. It can be concluded that the B20 blend achieved good thermal homogeneity, comparable to that of Jet A1 at the combustor outlet.

These findings indicate that WLOR2 can be effectively integrated into conventional aviation fuel systems without significantly modifying existing combustor designs. Waste management and energy recovery are two industrial benefits that can be achieved through the use of recycled waste lubricating oil in fuel blends. Industries that rely on liquid fuels, like aviation, power generation, or industrial burners, may find WLOR2 to be a viable option due to its compatibility with Jet A1.

However, further investigation is warranted to comprehensively evaluate emissions, including soot, unburned hydrocarbons (UHC), and nitrogen oxides (NO_x) to facilitate wider adoption. Additionally, optically visualizing the flame characteristics is highly recommended to gain deeper insights into the combustion behavior of WLOR2/Jet A1 blends. Such assessments would not only enhance the understanding of the fundamental combustion processes but also facilitate the identification of potential challenges and opportunities associated with the commercial application of WLOR2 as a fuel in combustion systems, such as industrial burners. These

efforts could pave the way for optimizing the performance and environmental compatibility of WLOR2-based fuels in practical applications.

CRediT authorship contribution statement

Ahmed I. EL-Seesy: Writing – review & editing, Writing – original draft, Resources, Methodology, Investigation, Formal analysis, Data curation, Conceptualization. **Ahmed S. Attia:** Writing – review & editing, Writing – original draft, Investigation, Formal analysis. **Radwan M. EL-Zohairy:** Writing – review & editing, Writing – original draft, Methodology, Investigation, Formal analysis. **Mohamed I. Hassan Ali:** Writing – review & editing, Writing – original draft, Visualization, Supervision, Funding acquisition.

Declaration of competing interest

The authors declare that they have no known competing financial interests or personal relationships that could have appeared to influence the work reported in this paper.

Acknowledgments

This research was supported by Khalifa University (Grant No. RIG 2023-091).

Data availability

Data will be made available on request.

References

[1] O. Arpa, R. Yumrutaş, Ö. Kaşka, Desulfurization of diesel-like fuel produced from waste lubrication oil and its utilization on engine performance and exhaust emission, Appl. Therm. Eng. 58 (2013) 374–381, https://doi.org/10.1016/j.applthermaleng.2013.04.035.
[2] A. Santhoshkumar, A. Ramanathan, Recycling of waste engine oil through pyrolysis process for the production of diesel like fuel and its uses in diesel engine, Energy 197 (2020), https://doi.org/10.1016/j.energy.2020.117240.
[3] C. Kassargy, S. Awad, G. Burnens, K. Kahine, M. Tazerout, Gasoline and diesel-like fuel production by continuous catalytic pyrolysis of waste polyethylene and polypropylene mixtures over USY zeolite, Fuel 224 (2018) 764–773, https://doi.org/10.1016/j.fuel.2018.03.113.
[4] M. Gear, J. Sadhukhan, R. Thorpe, R. Clift, J. Seville, Abstract, J. Clean. Prod. (2018), https://doi.org/10.1016/j.jclepro.2018.01.015.
[5] S. Li, S. Xu, S. Liu, C. Yang, Q. Lu, Fast Pyrolysis of Biomass in free-fall Reactor for hydrogen-rich Gas, vol. 85, 2004, pp. 1201–1211, https://doi.org/10.1016/j.fuproc.2003.11.043.
[6] R. Zanzi, K. Sjstrm, E. Bjrnbom, Rapid high-temperature Pyrolysis of Biomass in a free-fall Reactor, vol. 75, 1996, pp. 545–550.
[7] C. Ilk, Optimization of Fuel Production from Waste Vehicle Tires by Pyrolysis and Resembling to Diesel Fuel by Various Desulfurization Methods, vol. 102, 2012, pp. 605–612, https://doi.org/10.1016/j.fuel.2012.06.067.
[8] P. Azadi, O.R. Inderwildi, R. Farnood, D.A. King, Liquid fuels , hydrogen and chemicals from lignin : a critical review, Renew. Sustain. Energy Rev. 21 (2013) 506–523, https://doi.org/10.1016/j.rser.2012.12.022.
[9] J. Akhtar, N. Saidina Amin, A review on operating parameters for optimum liquid oil yield in biomass pyrolysis, Renew. Sustain. Energy Rev. 16 (2012) 5101–5109, https://doi.org/10.1016/j.rser.2012.05.033.
[10] F. Abnisa, W.M.A. Wan Daud, S. Ramalingam, M.N.B.M. Azemi, J.N. Sahu, Co-pyrolysis of palm shell and polystyrene waste mixtures to synthesis liquid fuel, Fuel 108 (2013) 311–318, https://doi.org/10.1016/j.fuel.2013.02.013.
[11] V.I. Sharypov, N. Marin, N.G. Beregovtsova, S.V. Baryshnikov, B.N. Kuznetsov, V.L. Cebolla, J.V. Weber, Co-pyrolysis of wood biomass and synthetic polymer mixtures. Part I: influence of experimental conditions on the evolution of solids, liquids and gases, J. Anal. Appl. Pyrolysis 64 (2002) 15–28, https://doi.org/10.1016/S0165-2370(01)00167-X.
[12] A. Gunerhan, O. Altuntas, H. Caliskan, Analyzing the influence of feedstock selection in pyrolysis on aviation gas turbine engines: a study on performance, combustion efficiency, and emission profiles, Energy 306 (2024), https://doi.org/10.1016/j.energy.2024.132513.
[13] Y. Castillo Santiago, A. Martínez González, O.J. Venturini, L.A. Sphaier, E.A. Ocampo Batlle, Energetic and environmental assessment of oil sludge use in a gasifier/gas microturbine system, Energy 244 (2022), https://doi.org/10.1016/j.energy.2022.123103.
[14] T. Suchocki, Witanowski, P. Lampart, P. Kazimierski, K. Januszewicz, B. Gawron, Experimental investigation of performance and emission characteristics of a miniature gas turbine supplied by blends of kerosene and waste tyre pyrolysis oil, Energy 215 (2021), https://doi.org/10.1016/j.energy.2020.119125.
[15] S. Wang, D.A. Rodriguez Alejandro, H. Kim, J.Y. Kim, Y.R. Lee, W. Nabgan, B.W. Hwang, D. Lee, H. Nam, H.J. Ryu, Experimental investigation of plastic waste pyrolysis fuel and diesel blends combustion and its flue gas emission analysis in a 5 kW heater, Energy 247 (2022), https://doi.org/10.1016/j.energy.2022.123408.
[16] M. Broumand, M.S. Khan, S. Yun, Z. Hong, M.J. Thomson, Feasibility of running a micro gas turbine on wood-derived fast pyrolysis bio-oils: effect of the fuel spray formation and preparation, Renew. Energy 178 (2021) 775–784, https://doi.org/10.1016/j.renene.2021.06.105.
[17] T. Seljak, S. Rodman Oprešnik, T. Katrašnik, Microturbine combustion and emission characterization of waste polymer-derived fuels, Energy 77 (2014) 226–234, https://doi.org/10.1016/j.energy.2014.07.020.
[18] M.C. Chiong, C.T. Chong, J.H. Ng, S.S. Lam, M.V. Tran, W.W.F. Chong, M.N. Mohd Jaafar, A. Valera-Medina, Liquid biofuels production and emissions performance in gas turbines: a review, Energy Convers. Manag. 173 (2018) 640–658, https://doi.org/10.1016/j.enconman.2018.07.082.
[19] M. Broumand, S. Albert-Green, S. Yun, Z. Hong, M.J. Thomson, Spray combustion of fast pyrolysis bio-oils: applications, challenges, and potential solutions, Prog. Energy Combust. Sci. 79 (2020), https://doi.org/10.1016/j.pecs.2020.100834.
[20] M. Shahbaz, N. Rashid, J. Saleem, H. Mackey, G. McKay, T. Al-Ansari, A review of waste management approaches to maximize sustainable value of waste from the oil and gas industry and potential for the State of Qatar, Fuel 332 (2023), https://doi.org/10.1016/j.fuel.2022.126220.
[21] M. Calero, R.R. Solís, M.J. Muñoz-Batista, A. Pérez, G. Blázquez, M. Ángeles Martín-Lara, Oil and gas production from the pyrolytic transformation of recycled plastic waste: an integral study by polymer families, Chem. Eng. Sci. 271 (2023) 118569, https://doi.org/10.1016/j.ces.2023.118569.
[22] R.M. El-Zoheiry, A.I. EL-Seesy, A.M.A. Attia, Z. He, H.M. El-Batsh, Combustion and emission characteristics of jojoba biodiesel-jet A1 mixtures applying a lean premixed pre-vaporized combustion techniques: an experimental investigation, Renew. Energy 162 (2020) 2227–2245, https://doi.org/10.1016/j.renene.2020.10.031.
[23] S.J. Kline, The purposes of uncertainty analysis, J. Fluid. Eng. Trans. ASME 107 (1985) 153–160, https://doi.org/10.1115/1.3242449.

[24] S.S. Lam, A.D. Russell, C.L. Lee, H.A. Chase, Microwave-heated pyrolysis of waste automotive engine oil: influence of operation parameters on the yield, composition, and fuel properties of pyrolysis oil, Fuel 92 (2012) 327–339, https://doi.org/10.1016/j.fuel.2011.07.027.
[25] R. Maceiras, V. Alfonsín, F.J. Morales, Recycling of waste engine oil for diesel production, Waste Manag. 60 (2017) 351–356, https://doi.org/10.1016/j.wasman.2016.08.009.
[26] M.L. Fernández-Sánchez, M.T. Fernández-Arguelles, J.M. Costa-Fernández, Optical atomic emission spectometry/flame photometry, Ref. Mod. Chem/, Mol. Sci. Chem. Eng. (2018) 160–168, https://doi.org/10.1016/B978-0-12-409547-2.14533-0.
[27] M.S.A. Malik, A.I. Mohamad Shaiful, M.S. Mohd Ismail, M.N. Mohd Jaafar, A.M. Sahar, Combustion and emission characteristics of coconut-based biodiesel in a liquid fuel burner, Energies 10 (2017) 1–12, https://doi.org/10.3390/en10040458.
[28] S. Senthur Prabu, M.A. Asokan, R. Roy, S. Francis, M.K. Sreelekh, Performance, combustion and emission characteristics of diesel engine fuelled with waste cooking oil bio-diesel/diesel blends with additives, Energy 122 (2017) 638–648, https://doi.org/10.1016/j.energy.2017.01.119.
[29] M. Kumar, C. Tung Chong, S. Karmakar, Comparative assessment of combustion characteristics of limonene, Jet A-1 and blends in a swirl-stabilized combustor under the influence of pre-heated swirling air, Fuel 316 (2022) 123350, https://doi.org/10.1016/j.fuel.2022.123350.
[30] M.C. Chiong, C.T. Chong, J.H. Ng, S.S. Lam, M.V. Tran, W.W.F. Chong, M.N.M. Jaafar, A. Valera-Medina, Liquid biofuels production and emissions performance in gas turbines: a review, Energy Convers. Manag. 173 (2018) 640–658, https://doi.org/10.1016/j.enconman.2018.07.082.
[31] Y. Gao, J. Deng, C. Li, F. Dang, Z. Liao, Z. Wu, L. Li, Experimental study of the spray characteristics of biodiesel based on inedible oil, Biotechnol. Adv. 27 (2009) 616–624, https://doi.org/10.1016/j.biotechadv.2009.04.022.
[32] A.H. Lefebvre, D.R. Ballal, Gas Turbine Combustion: Alternative Fuels and Emissions, CRC press, 2010.
[33] E. Sann, M. Anwar, R. Adnan, M.A. Idris, Biodiesel for gas turbine application — an atomization characteristics study, in: Advances in Internal Combustion Engines and Fuel Technologies, InTech, 2013, https://doi.org/10.5772/54154.
[34] S.W. Park, S. Kim, C.S. Lee, Breakup and atomization characteristics of mono-dispersed diesel droplets in a cross-flow air stream, Int. J. Multiphas. Flow 32 (2006) 807–822, https://doi.org/10.1016/j.ijmultiphaseflow.2006.02.019.
[35] S. Kim, J.W. Hwang, C.S. Lee, Experiments and modeling on droplet motion and atomization of diesel and bio-diesel fuels in a cross-flowed air stream, Int. J. Heat Fluid Flow 31 (2010) 667–679, https://doi.org/10.1016/j.ijheatfluidflow.2010.02.001.
[36] C.E. Ejim, B.A. Fleck, A. Amirfazli, Analytical study for atomization of biodiesels and their blends in a typical injector: surface tension and viscosity effects, Fuel 86 (2007) 1534–1544, https://doi.org/10.1016/j.fuel.2006.11.006.
[37] O. Arpa, R. Yumrutaş, Z. Argunhan, Experimental investigation of the effects of diesel-like fuel obtained from waste lubrication oil on engine performance and exhaust emission, Fuel Process. Technol. 91 (2010) 1241–1249, https://doi.org/10.1016/j.fuproc.2010.04.004.
[38] O. Arpa, R. Yumrutaş, Ö. Kaşka, Desulfurization of diesel-like fuel produced from waste lubrication oil and its utilization on engine performance and exhaust emission, Appl. Therm. Eng. 58 (2013) 374–381, https://doi.org/10.1016/j.applthermaleng.2013.04.035.
[39] S. Muhbat, F. Suleman, S.M.A. Jilani, S.A.A. Taqvi, A. Borhan, F. Khan, T. Alshahrani, F. Ahmad, Production of diesel-like fuel by catalytic co-pyrolysis of waste cooking oil and waste lubricating oil—an alternate energy source, Biomass Convers Biorefin (2024), https://doi.org/10.1007/s13399-024-06183-z.